Scientific Research Communications

Research Article

Sci. Res. Comm. (2024)
Volume 4, Issue 2
doi: 10.52460/src.2024.009

Finite Element Analysis of Delamination Initiation in Wind Turbine Blade Spar Caps: Role of Compression, Strain Energy, and Principal Stresses

Ferhat Özmen[1,*] Ramazan Karakuzu[1]

[1] Dokuz Eylül University, Faculty of Engineering, Department of Mechanical Engineering, İzmir
[*] Corresponding author: ferhatozmen35@gmail.com

Received: 07.07.2024 Accepted: 05.08.2024

Abstract

In wind turbine blades, utilizing the finite element method (FEM) to identify potential failure modes before production provides considerable value and cost savings in contrast to conventional structural tests. This paper focuses on examining the factors leading to delamination in spar caps and exploring the initiation of this delamination using the finite element method. Compression, total strain energy density, and principal stresses are significant among the variables examined to determine the effects on model deformation and crack formation. Examining these variables may contribute to understanding the mechanisms involved in initiating and progressing delamination. This study examined the effects of compression, total strain energy density, and principal stresses on model deformation and crack formation. This study focuses on the effects of principal stresses on displacement, the effects of compression on delamination and crack formation, and the effects of total strain energy density on fracture tendency and failure modes due to delamination.

Keywords: Spar cap, finite element method, compression, strain energy density, principal stress, crack formation, delamination, buckling

1. Introduction

The utilization of the finite element method (FEM) in the evaluation of potential failure modes in wind turbine blades presents a paradigm shift in the industry, offering substantial cost savings and enhanced predictive capabilities compared to conventional structural tests. Investigating failure initiation and progression through numerical simulations prior to advancing to blade production and structural testing represents a highly critical and advantageous approach. This methodology, developed through studies that have made significant contributions to the literature, is essential to ensure that the design of wind turbine blades maintains structural integrity and provides a partial validation of these designs.

Overgaard and Lund (2010) investigated the structural collapse of a wind turbine blade and determined that the collapse was caused by multiple local buckling-induced delamination processes. They identified that delamination between the spar layers led to buckling damage, resulting in the structural failure of the blade. To observe composite delamination, they defined a cohesive zone between the layers. They emphasized the need for guidelines and recommendations to accurately assess delamination in wind turbine blades. Branner and Berring (2011) investigated the behavior of delamination in rectangular composite panels with initial delamination under compressive loading. By comparing experimental findings with a numerical parameter study, they created a buckling mode map for panels similar to the load-bearing flange in the main spar of a wind turbine blade. The study showed that the shape of the buckling mode depends on the thickness, size, and location of the delamination. Yang et al. (2012) studied the failure of a 40-meter wind turbine blade and, based on full-scale test results, demonstrated that the primary cause of the blade's failure was the separation of adhesive surfaces. Chen et al. (2014) conducted a full-scale failure test on a 52.3-meter wind turbine blade and identified that delamination in the spar caps and damage in the spar webs at the root transition zone were the primary mechanisms leading to the blade's failure. Local buckling facilitates out-of-plane deformation, contributing to this damage mechanism. Additionally, it was concluded that the thickness-direction stresses causing adhesive separation and delamination in the root transition zone of large blades should be considered in finite element analysis. Subsequently, Chen et al. (2015) investigated the local buckling strength of a 10.3-meter wind turbine blade and found, through finite element analysis, that sharp-edged blade configurations exhibited less resistance to local buckling. During testing, local buckling was observed in the spar webs and shell surfaces; however, no composite laminate failure was noted in these areas. These findings suggest the potential for different failure mechanisms across varying blade sizes. Haselbach and Branner (2016) examined the buckling behavior at the trailing edge during static tests of a 34-meter-long blade and its impact on the blade's strength. As a result of this investigation, an innovative technique incorporating a cohesive zone to model the adhesive surface at the trailing edge was proposed. Muyan and Çöker (2020), compared the static and fatigue strengths of an adhesive-separated RÜZGEM blade and an undamaged blade under flap-wise loading using numerical analyses. The results showed that the strength of the RÜZGEM blade with adhesive failure significantly decreased compared to the undamaged blade under both static and fatigue loadings.

This study revisits two significant contributions to the literature by applying advanced methods from finite element simulation programs within a specific scope and presents new findings. Batmaz et al. (2021) examined the finite element model of the RÜZGEM 5-meter glass fiber reinforced polymer wind turbine blade, whose spar cap is made of different composite layers, under the minimum flapwise load, the adhesive separation failure based on the cohesive zone model at the high pressure shell side-spar interface. The adhesive separation failure occurring at the specified load level was found not to adversely affect the structural integrity of the blade in a catastrophic manner. Haselbach (2015) investigated an 8.65-meter-long blade section with different initial delamination in the main spar by applying a cantilever bending moment. In this blade model, where the spar cap is entirely unidirectional (UD), local buckling caused high stresses and strains around the delamination, potentially exceeding the material's design properties and making failure initiation and progression more likely.

This paper meticulously examines the variables influencing model deformation and crack initiation, emphasizing the critical roles of compression, total strain energy density, and principal stresses. By elucidating these dynamics, the research aims to provide a deeper understanding of delamination initiation and progression, offering valuable insights for optimizing blade design and enhancing structural integrity. The investigation focuses on the consequences of principal stresses on displacement, the impact of compression on delamination and crack formation, and the influence of total strain energy density on fracture propensity and delamination-induced failure modes. In general, tensile stress is prevalent at the intersection of the spar cap and blade root in spar caps and blades, while compressive stress is predominant in the remaining parts. This is attributed to the bending force applied by the spar cap to support the blade and the pressure differentials on the blade surface caused by wind. Compressive stresses help mitigate crack formation and propagation. It is crucial for the blade areas experiencing significantly higher tensile stress than compressive stress to possess more excellent resistance. Otherwise, the blade may be susceptible to breaking or cracking at this location. Total strain energy density (TSED) values indicate the area where a crack will occur. In the case of adhesive separation of a material, TSED values often reach maximum values. In this way, the regions where TSED values are maximum indicate the places where adhesive separation will begin. TSED is essential in material failure analysis, identifying critical crack formation or growth regions, and estimating structural strength. Wind-induced pressure produces material stresses as principal stresses, which are the main factors that cause the buckling of spar caps. Local buckling in the delamination region under the influence of principal stresses may cause the central area of the delamination to be subjected to different stresses in different directions, resulting in stress concentration. As a result, stress concentration occurs at the delamination boundary due to principal stresses along the bending direction of the laminate. The concentration of principal stresses is a potential failure zone for the adhesive element. If the principal stresses exceed the strength of the cohesive member, the cohesive member will rupture, and the two connected parts will separate.

This study used two wind turbine blade models to examine delamination initiation criteria: the RUZGEM 5-meter wind turbine blade as the first blade model (Batmaz et al., 2021) and the DTU 10 MW wind turbine blade as the second model (Haselbach, 2015).

2. Finite Element Analysis Details

2.1. Materials of RUZGEM 5-m Wind Turbine Blade Model

In assembling the finite element model of the RÜZGEM 5-meter blade, the design of the composite laminates and the blade structure for the root and trailing edge/spar web panels considered four different materials. Specifically, two types of glass fabric (Triax and UD), steel, and polymeric foam (Divinycell H45) were used as core materials for the sandwich structures (Table 1).

Table 1. Material properties of RUZGEM 5-m Wind Turbine Blade Model

Materials/Engineering Constants	Density (kg/m^3)	Modulus (GPa)	Strength (MPa)	Poisson Ratio
Lamina (Triax)	1896	E_1= 24.84 E_2= 9.14 G_{12}=2.83	S_{XT} = 191.73 S_{XC} = 101.16 S_{YT} = 16.86 S_{YC} = 50.41 S_{SH} = 11.29	0.29
Steel	7850	E= 210	S=581.80	0.30
Gelcoat	1200	E= 3.98	S=35.29	0.34
CSM 300 (UD)	1896	E= 9.14	S=16.86	0.29
Divinycell H45 (Foam)	48	E_1= 55E-03 E_2= 55E-03 G_{12}= 15E-03	S_T =1.40 S_C =0.60 S_{SH} =0.56	0.40
Adhesive	1400	E= 3.00 G_{12}= 1.59	S= 7.8	0.30

2.2. Contact Status of RUZGEM 5-m Wind Turbine Blade Model

In the predicted adhesive separation failure area, the cohesive zone was defined with adhesive models (Figure 1). Glue contact was preferred so that the connection between the adhesive and composite parts is suitable for the multi-point constraint method (Batmaz et al., 2021). In this study, a new investigation was conducted using the Glue Breaking effect instead of the MPC algorithm in MSC Marc/Mentat.

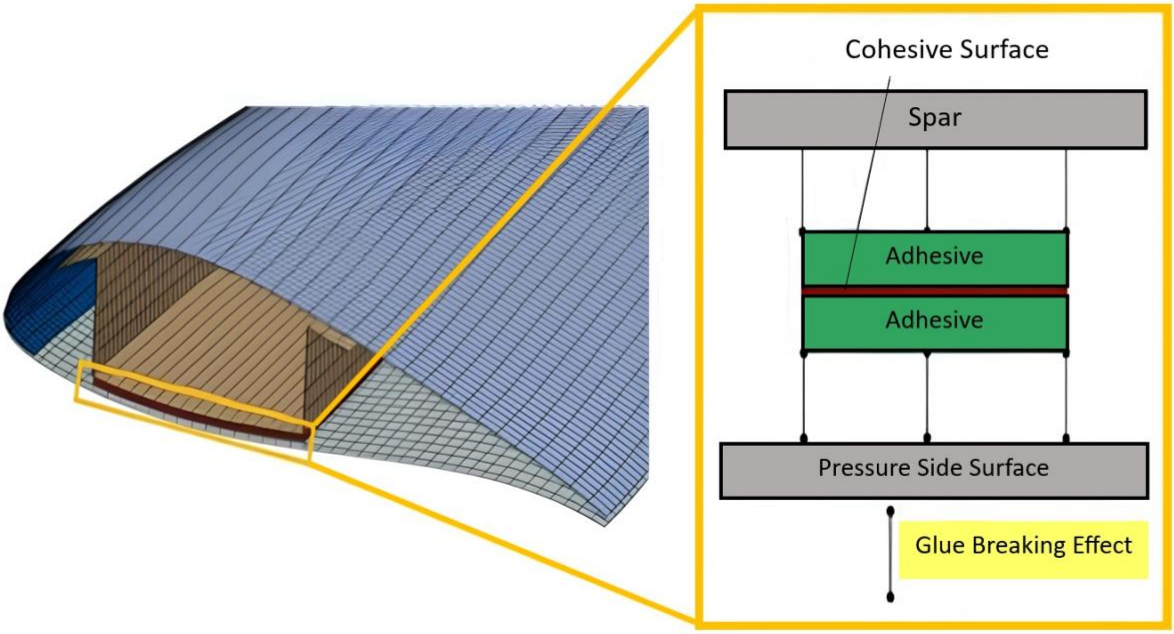

Figure 1. Schematic of the adhesive model (Batmaz et al., 2021)

2.3. Boundary Conditions of RUZGEM 5-m Wind Turbine Blade Model

In the first blade analysis study, as RUZGEM 5-m wind turbine blade and its spar cap, the adhesive region with 3D solid elements was created to connect the pressure side and two shell structures, such as a spar cap. The RUZGEM 5-m wind turbine blade is fixed at the blade root, and the spar cap supports the blade with adhesive bonding. The wind load on the blade exposed to 10 m/s wind speed was simulated and the blade root section is fixed as the boundary condition. The pressure distribution on the blade was first calculated using the MSC Cradle due to the wind flow. The material safety coefficient is accepted as 2.5. The number of shell elements and nodes is approximately 60 thousand, and the element sizes are generally around 15 mm. The material model in the finite element model created using the blade was verified through modal analysis in MSC Apex finite element software. Nonlinear static and buckling analyses were performed in MSC Marc/Mentat (Figure 2, Figure 3) (Batmaz et al., 2021).

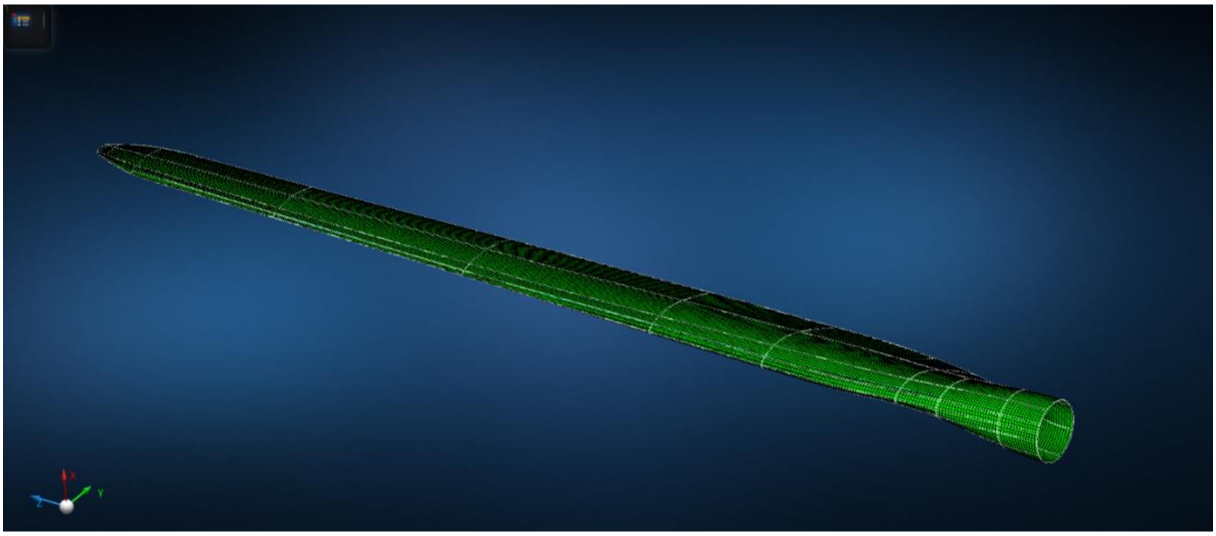

Figure 2. RUZGEM 5-m wind turbine blade

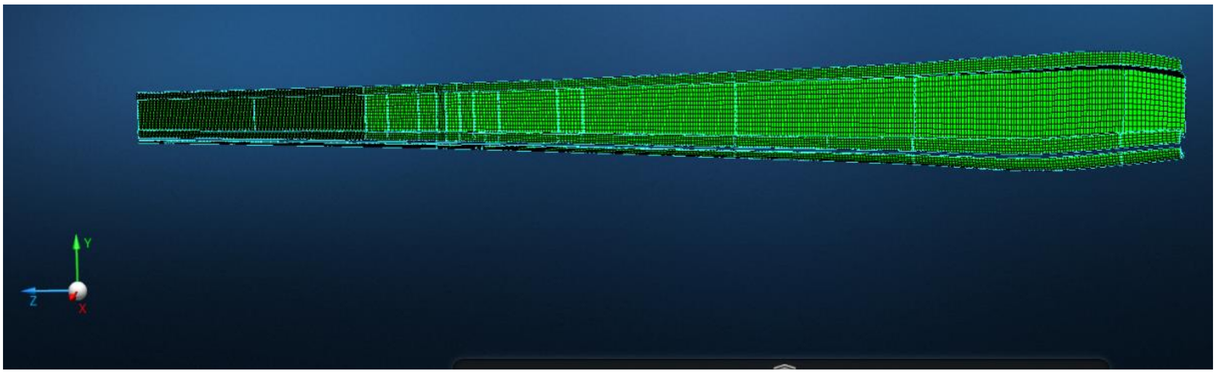

Figure 3. Spar cap of RUZGEM 5-m wind turbine blade

2.4. Materials of DTU 10 MW Wind Turbine Blade Model

The required materials and configurations were obtained from tables and graphs for the DTU 10 MW wind turbine blade section (Table 2). The outer surface of the blade was utilized as the reference surface containing the finite element nodes. The complete arrangement and material properties of the blade are available online (Bak et al., 2013). The spar cap of the DTU 10 MW wind turbine blade is composed of layers made entirely of UD material, arranged in a uniform configuration (Figure 4).

Table 2. Material properties of DTU 10MW Wind Turbine Blade

Engineering Constants	E_{11} (GPa)	E_{22} (GPa)	v_{12}	X^T (MPa)	X^C (MPa)	Y^T (MPa)	Y^C (MPa)	S^L	S^T	ρ (kg/m^3)
U/D Glass	41.26	11.39	0.33	903.6	660.16	42.14	42.14	58.65	58.65	1931

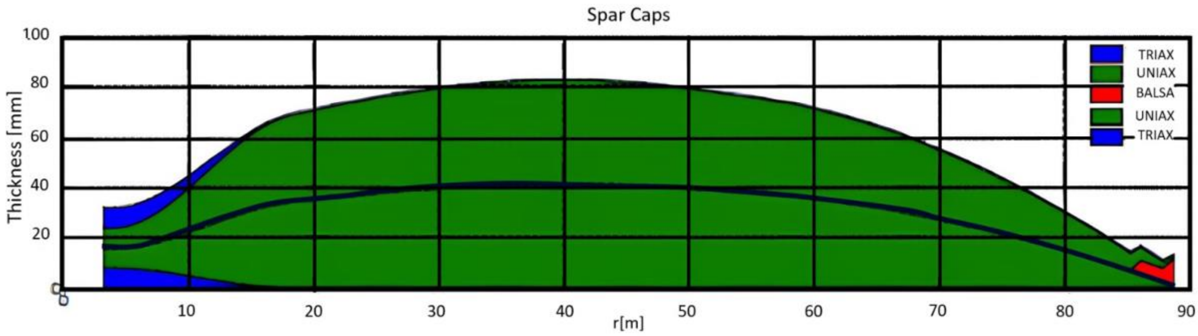

Figure 4. Composite layout of the DTU 10 MW wind turbine blade regions: Spar cap thickness in the 40-50m range of from blade root to blade tip (Castro and Branner, 2021)

2.5. Contact Status of DTU 10 MW Wind Turbine Blade Model

A contact definition was not established for the spar cap and other structures of the DTU 10 MW wind turbine blade. Consequently, the blade was designed as a rigid structure, and simulation studies commenced accordingly.

2.6. Boundary Conditions of DTU 10 MW Wind Turbine Blade Model

In the second blade analysis study, the DTU 10 MW wind turbine blade and its spar cap, the shell model contains approximately 40,000 four-node shell elements. The typical element length in the model was 0.05m (Figure 5). All nodes representing the posterior section (closest to the root) were fully constrained. The front section nodes were connected to a reference node using a constraint known as a rigid link (RBE2), allowing the front section to function as a rigid body. The blade section near the root on the opposite side of where the moment was applied was fixed as a boundary condition (Figure 6). The connections at the trailing edge and cap/body were generally modeled without specifying specific geometric details at the connection points. Three moments were applied to the reference node at the front: Mx = −16.4e9 Nmm, My = 2.4e9 Nmm, and Mz= 0.32e9 Nmm. The moments correspond to approximately 100% of the design loads evaluated for the airfoil section at r = 48.775m (middle of the simulated airfoil section). Experimental studies on the compressive strength of thick composite panels have shown that the loading must be high before delamination propagation near the panels' center. The moment was applied to ensure delamination growth was included in all simulated cases, including a safety factor of 1.35 (Haselbach, 2015).

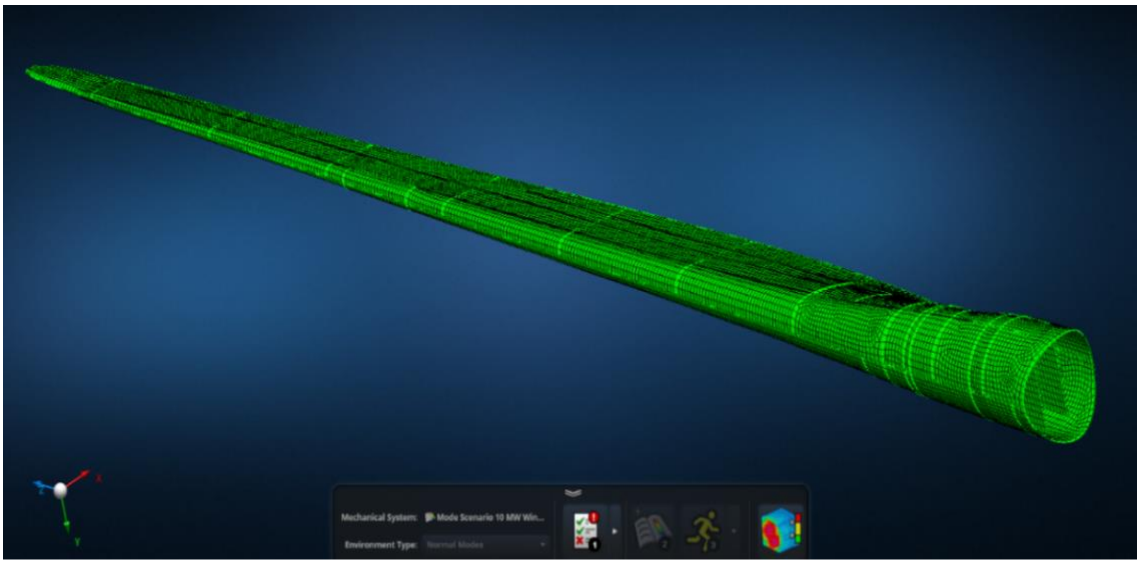

Figure 5. DTU 10 MW wind turbine blade (86-m)

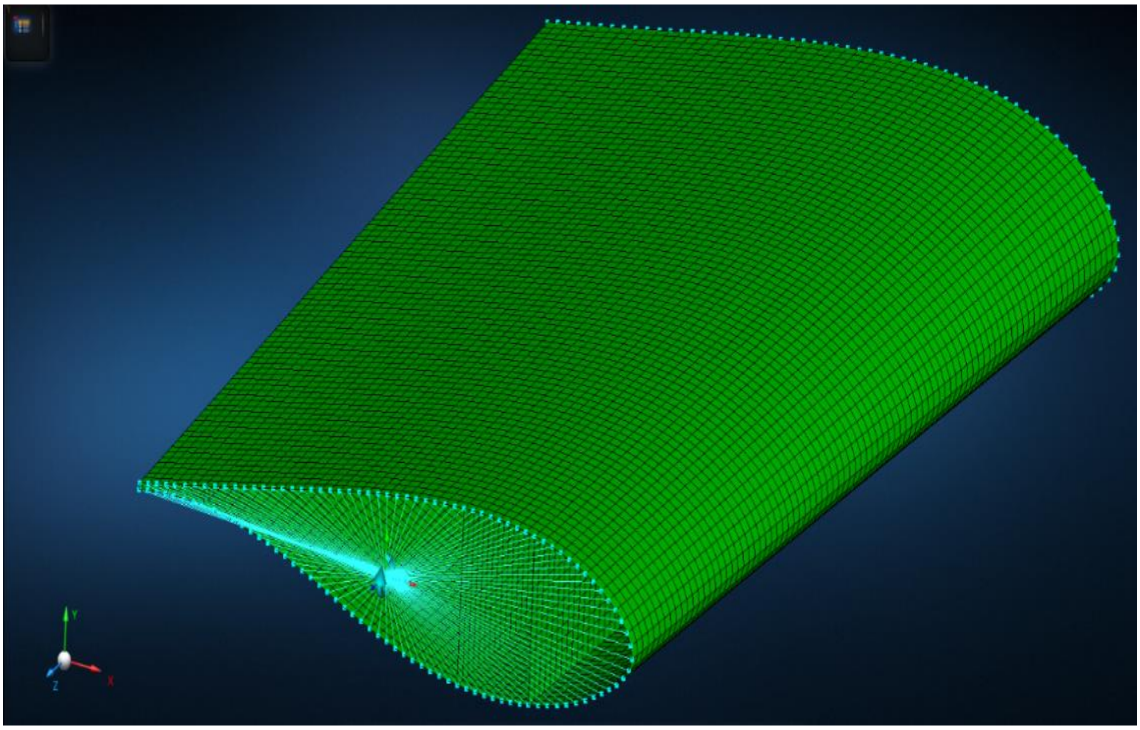

Figure 6. The blade section near the blade tip with applied moment (RBE2)

Mesh refinement was applied to the shell elements around the area of interest, where the initial delamination was modeled to reduce the characteristic element length to 0.01 m. The region surrounding the delamination was discretized using a fine mesh. The simulation applied the submodel method to simulate buckling-induced delamination growth in the spar cap (Mankins, 2023). The lower model was 1.7 m long and placed in the cap's center (Figure 7).

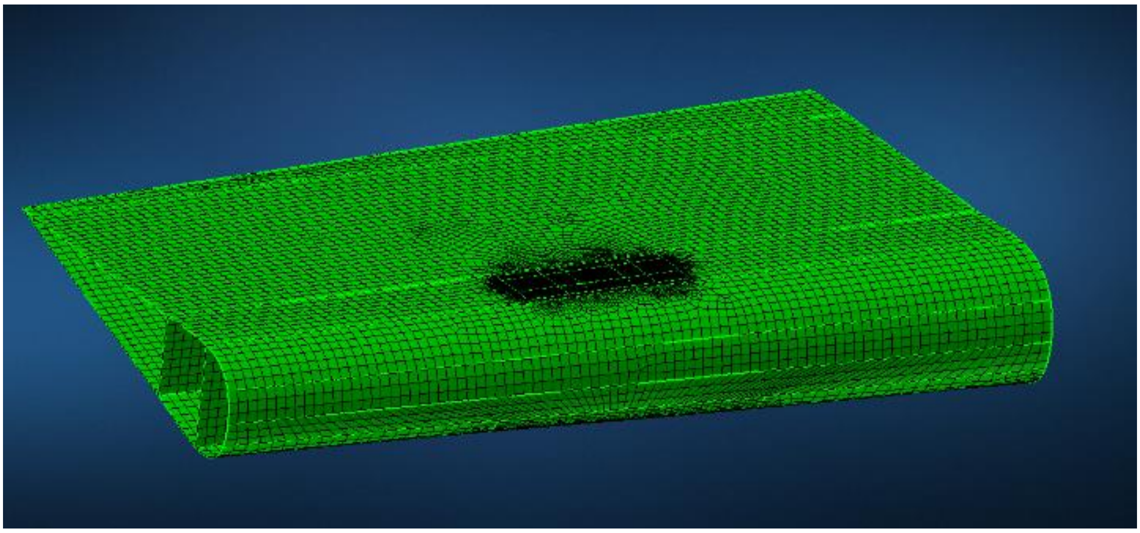

Figure 7. Blade section shell model of DTU 10MW wind turbine with mesh improvement

3. Results and Discussions

3.1. Role of Compression on RUZGEM 5-m Wind Turbine Blade Model

The tensile stress at the intersection of the spar cap and the blade root is much higher than the compressive stresses in the remaining part (Figure 8, Figure 9). There is a spar cap along the remaining part of the blade, but tensile stress is dominant only in the first part of the spar cap, where it intersects with the pressure side. This is because the bending force exerted by the spar cap to support the blade load is greater at the intersection of the blade root and the spar cap. The blade root is the thickest part; therefore, the most significant portion of the blade load is applied at this point. This causes a more significant bending moment where the spar cap intersects the blade root. This bending moment causes the spar cap to be pulled towards the blade root, resulting in tensile stresses. As a result, where the tensile stress in a spar cap of the blade is dominant, the bending force exerted by the spar cap to support the blade load is most significant. This is usually where the spar cap intersects the blade root.

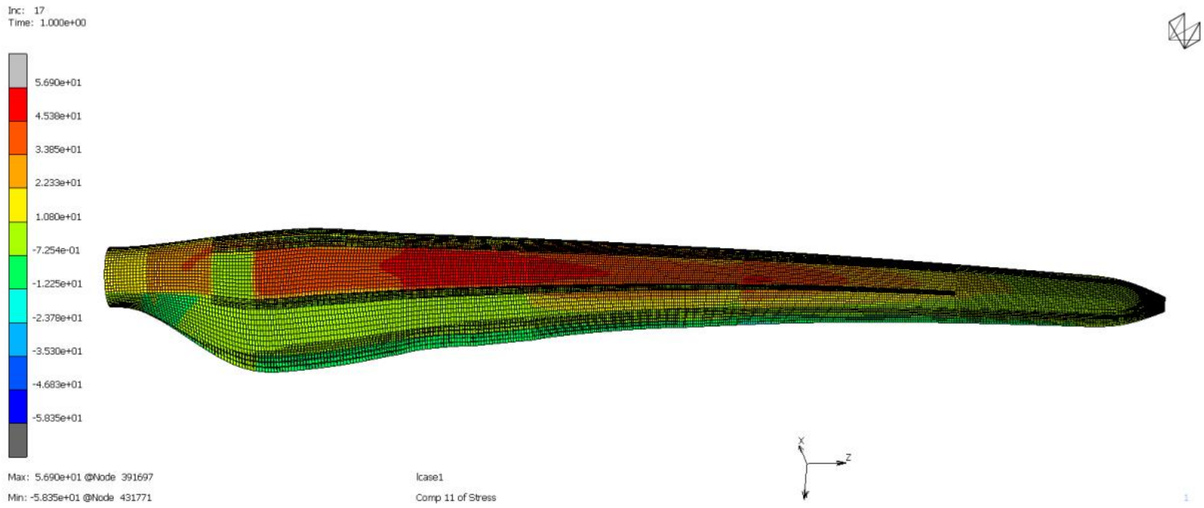

Figure 8. Compressive stress effect in the region where the material is expected to be subjected to a higher tension along 1 direction and the onset of adhesive failure is expected

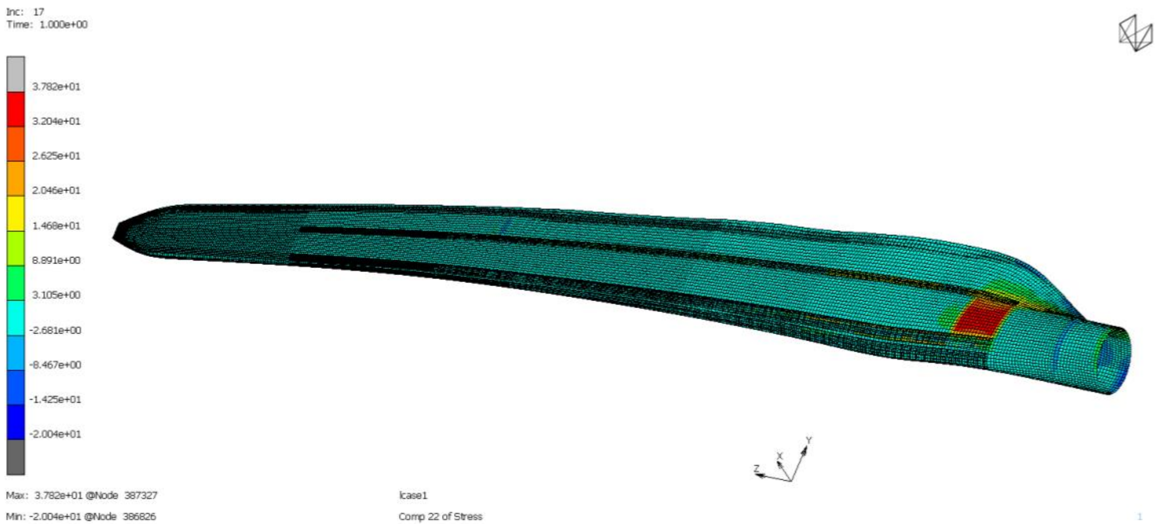

Figure 9. Tensile effect in the region where the material is expected to be exposed to a higher compression along 2 directions and the onset of adhesive failure

In general, tensile stress dominates at the intersection of the spar cap and blade root in spar caps and blades, while compressive stress dominates in the remaining part. This is due to the bending force exerted by the spar cap to support the blade and the pressure differences on the blade surface due to wind. There are several reasons why compressive stresses characterize this area:

1. In this intersection region, the spar cap separates from the pressure side, forming a bulge towards the suction side. This bulge creates a force center that causes compressive stresses on the suction side.

2. This region is subjected to blade bending at the blade root. When the blade is subjected to bending, compressive stresses occur on the suction side. This means that the blade root exerts a force towards the suction side.
3. This region is exposed to blade vibrations at the blade root. When the blade vibrates, compressive stresses occur on the suction side. This means that the blade root exerts a force towards the suction side.

Combining these three factors causes compressive stresses to dominate in this region. These compressive stresses can cause crack formation and material failure on the suction side. The intersection between the spar cap and the pressure side can be made smoother to reduce the stresses in this area. Additionally, measures can be taken to minimize blade bending and vibrations. This tensile force is much greater than the compressive stresses. As a result of this situation, the strength of the material at the intersection of the spar cap and the blade root must be higher than the strength of the material in the remaining part. Otherwise, the material may break or crack at this point. Where the spar cap intersects the blade root:

- Tensile stresses predominate.
- Tensile stresses are caused by the bending force exerted by the spar cap to support the blade load.
- Tensile stresses are much higher than compressive stresses.
- Compressive stresses are lower than tensile stresses at the intersection of the spar cap and the blade root.

Von Mises stress is defined as the square root of the mean of the squares of the three principal stress components of the material; therefore, von Mises stress indicates how close the material is to plastic deformation by combining the effects of the three principal stress components of the material (Figure 10).

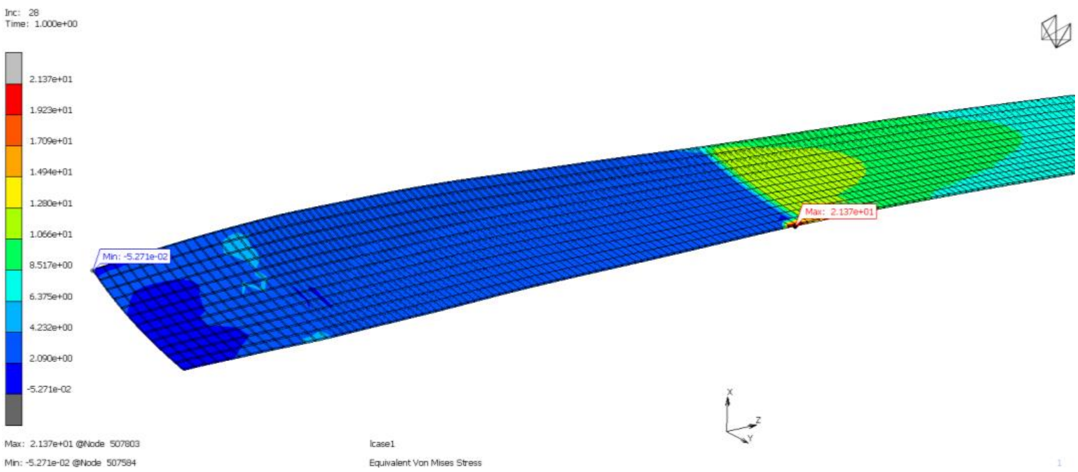

Figure 10. Equivalent of von Mises stresses

3.2. Role of Total Strain Energy Density on RUZGEM 5-m Wind Turbine Blade Model

Total strain energy density (TSED) is the strain energy stored in the unit volume of the material. Therefore, total strain energy indicates how much energy the material consumes during plastic deformation. The fact that the von Mises stress maximum point is slightly further away from the total strain energy density maximum point may suggest that the material is softer and more ductile at the other end of the region. In this case, even though the material in the area has a high von Mises stress, the total strain energy density will be low. To determine this situation more precisely, measurements of the material's properties, the applied load, and the form factor of the region are required.

The Crack Initiator method is a tool used to identify the initiation of a crack within a structure. No delamination or Turon method was used. The critical zone for cracks and structural failure is more likely to be in the area 1 meter further from the tip of the spar cap. The reason why no crack formation is observed in the section chosen as the crack initiation may be the compressive stresses and the total strain energy density. As a result, the difference in the regions where von Mises stress and total strain energy density are concentrated may be due to the difference in material properties, applied load, or form factor of the region. The bonding force between the layers and the adhesive bonding can be subjected to stresses that reduce the strength (Figure 11).

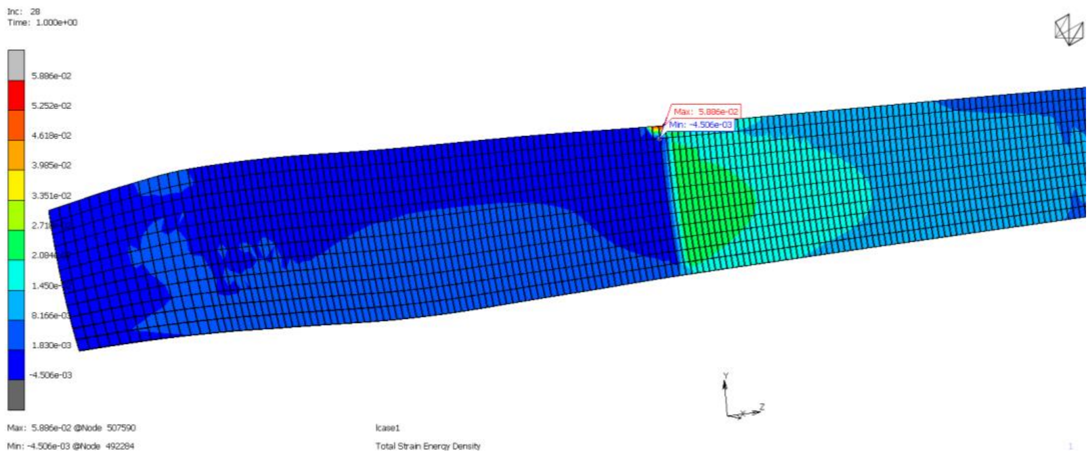

Figure 11. Total strain energy density and crack initiation

Total Strain Energy Density (TSED) values indicate the area where a crack will occur. These maximum values indicate the crack that will start when the adhesive separates. In the case of adhesive separation of a material, TSED values often reach maximum values. These maximum values represent the crack's location, which will initiate adhesive separation and the energy required for the crack to grow. In this way, the regions where TSED values are maximum indicate the places where adhesive separation will begin (Figure 12) (Branner and Berring, 2011).

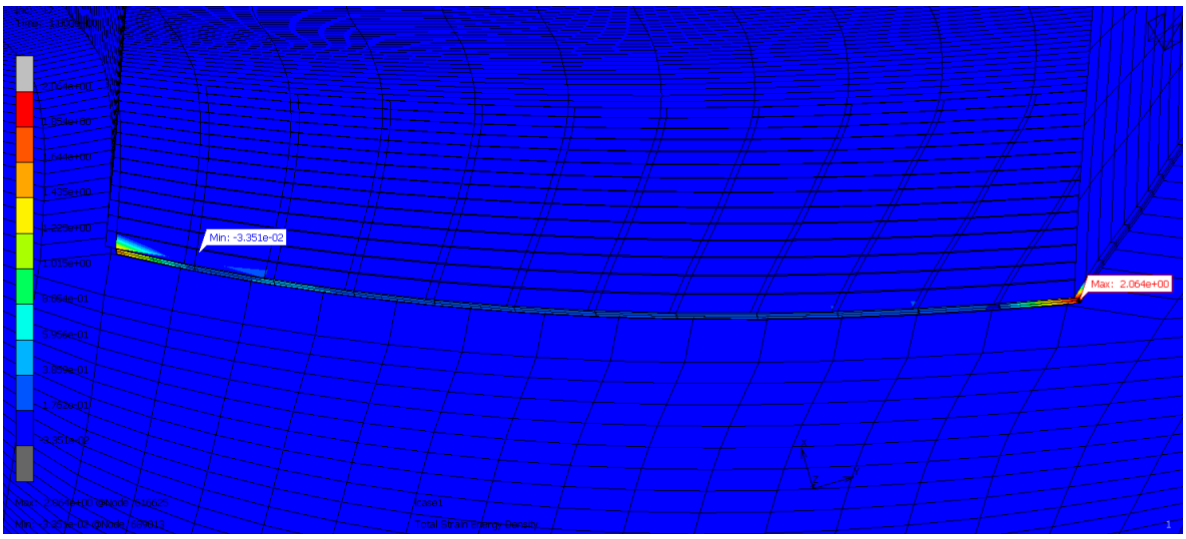

Figure 12. Total strain energy density in the adhesive region where failure is expected

TSED is essential in material failure analysis, identifying critical crack formation or growth regions, and estimating structural strength. These values can be determined through various material tests and simulations and used to understand the material's structural behavior (Figure 13).

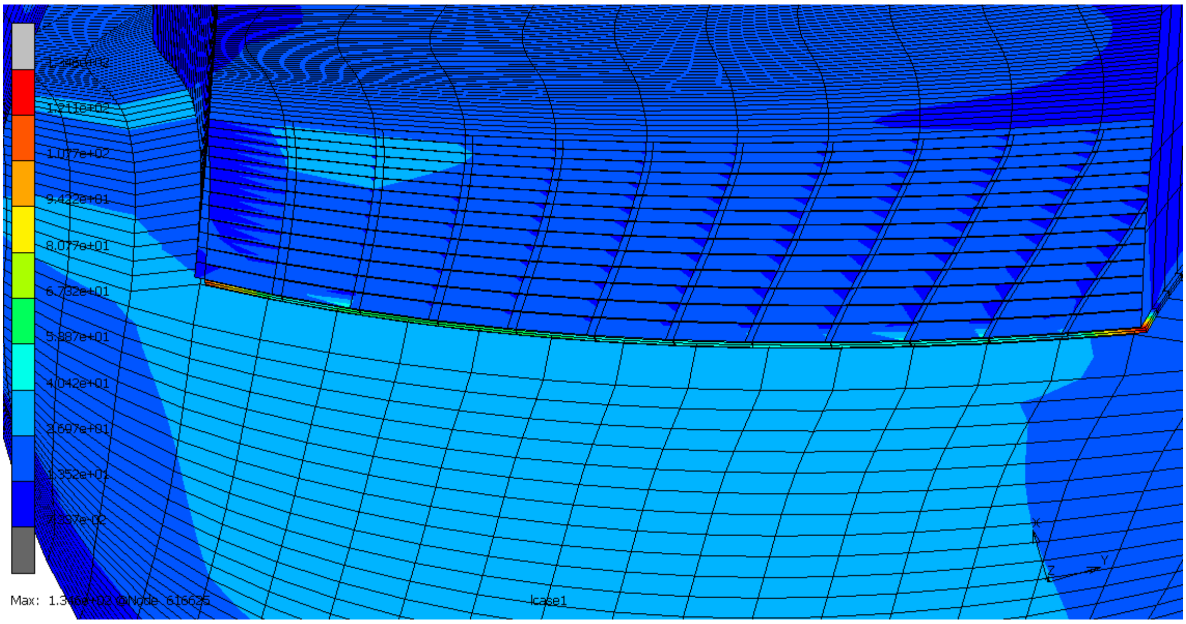

Figure 13. Stress distribution in the adhesive region where failure is expected

Crack formation is expected to occur more in the region where the total strain energy density is concentrated, and the Crack Initiator is generally assigned to these concentrated regions. It was observed that the contact status was eliminated both in the area where adhesive separation was expected and, in the part, where laminate breakage was expected (Figure 14).

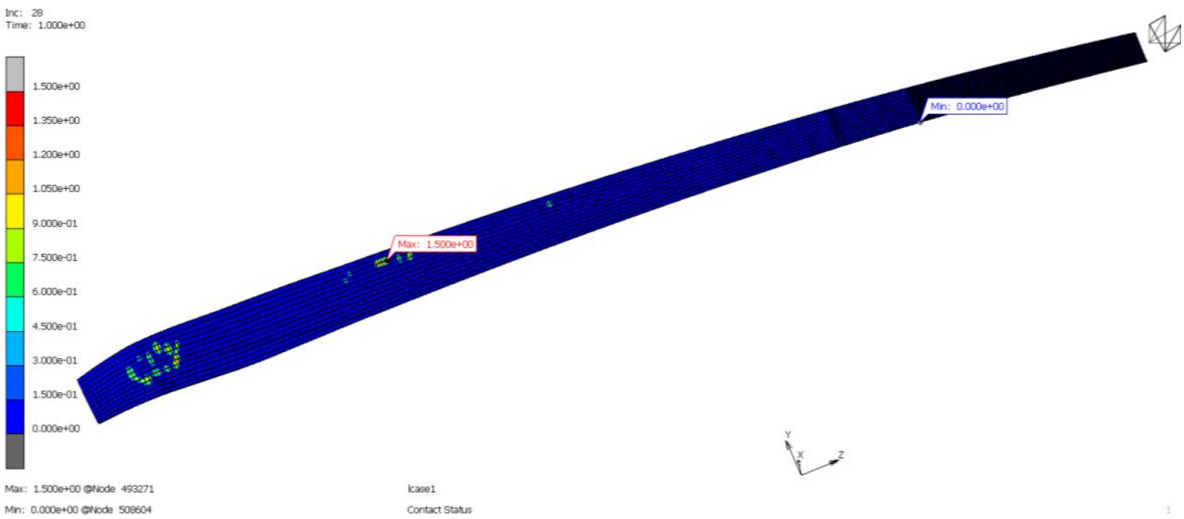

Figure 14. Contact status was eliminated both in the area as an adhesive separation and laminate breakage was expected

The spar cap region, which marks the beginning of delamination, was selected as the crack initiation site to examine the formation of cracks, fractures, and structural failure. No cracks were observed, possibly due to compression. Tensile stresses generally open cracks, while compressive stresses tend to close them. This suggests that delamination does not directly result in "fracture." Instead, it is just one of the factors that can lead to structural failure (Figure 15).

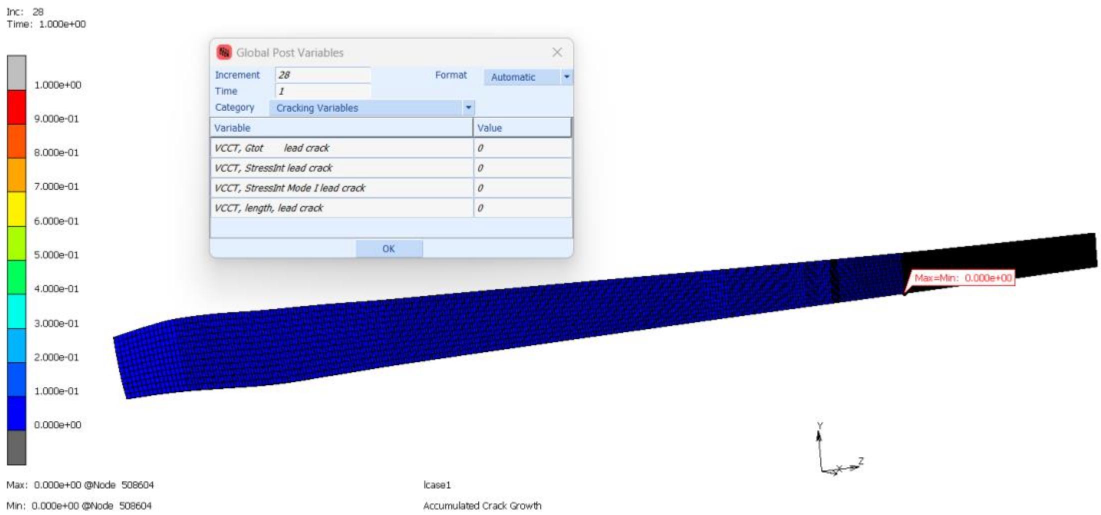

Figure 15. No crack growth

3.3. Role of Principal Stress on RUZGEM 5-m Wind Turbine Blade Model

Cohesive zone modeling (CZM) is a numerical technique to simulate fracture and delamination in materials and structures. It is a method employed to model the behavior that arises when two composite layers separate. This method is invaluable in analyzing structures subjected to loading conditions that may induce crack propagation. In cohesive zone model analysis, Element 149 is used as an 8-node solid composite element, 75 as a 4-node shell element, and 188 as the 8-node interface element. Various experiments were conducted, and VCCT and CZM methods were assessed to determine the potential for Glue Breaking effect (Figures 16, Figure 17). The Glue Breaking feature relies on regular Touch contact, which may involve friction and other properties when the criterion for breakage in the glue contact is reached (Table 3).

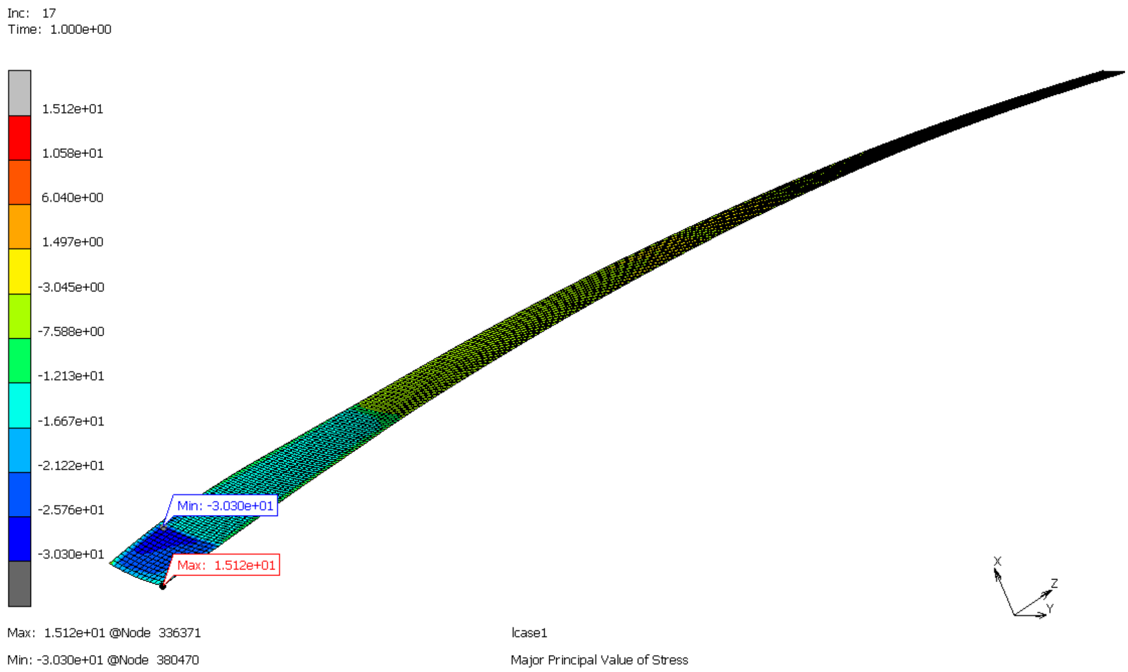

Figure 16. Minimum and maximum principal stresses - CZM (non-Glue Breaking)

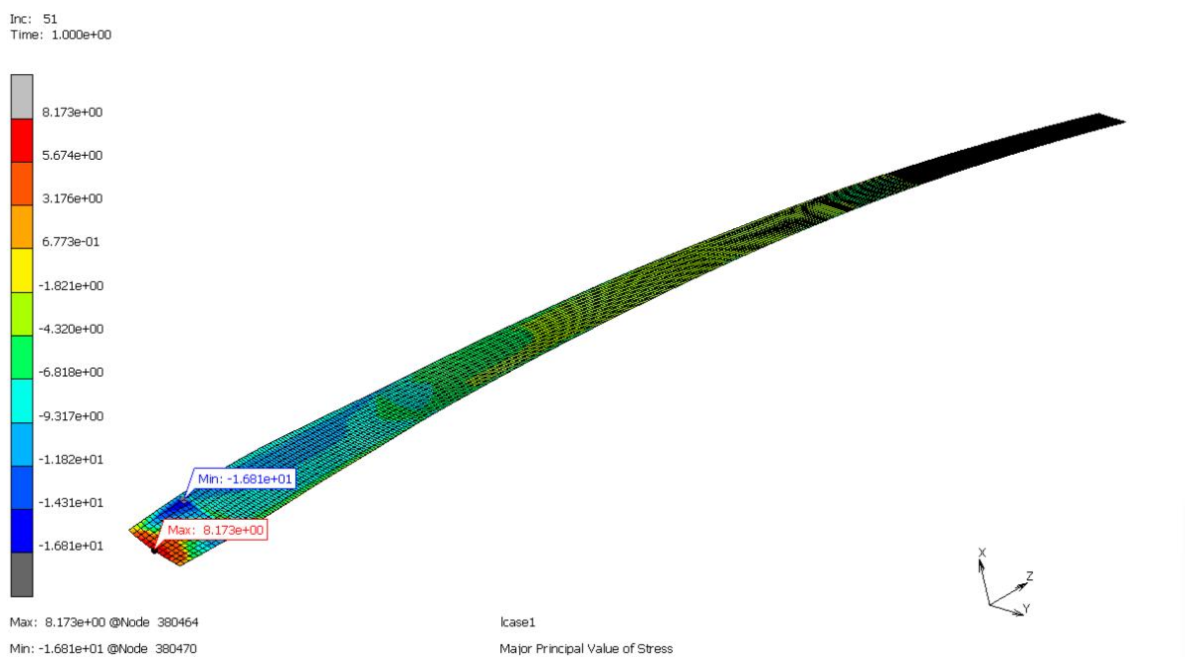

Figure 17. Minimum and maximum principal stresses - CZM (with Glue Breaking)

Table 3. Cohesive zone status

CZM (non-Glue Breaking)		CZM (with Glue Breaking)	
Type	Stress Values (MPa)	Type	Stress Values (MPa)
Max. Principal Stress	-30.30	Max. Principal Stress	8.2
Min. Principal Stress	15.1	Min. Principal Stress	-16.8

Virtual Crack Closure Technique (VCCT) is a powerful fracture mechanics tool that predicts the crack tip's strain energy release rate (SERR). It can be used with various material models, including linear elastic, elastic-plastic, and cohesive zone models. It is used for crack growth prediction, fracture toughness evaluation, or design optimization of cracked structures. Accuracy is reduced in CZM studies without Glue Breaking (Table 4), and CZM gives almost the same results as VCCT (Figure 18, Figure 19).

Table 4. VCCT failure status

VCCT (non-Glue Breaking)		VCCT (with Glue Breaking)	
Type	Stress Values (MPa)	Type	Stress Values (MPa)
Max. Principal Stress	-30.32	Max. Principal Stress	8.2
Min. Principal Stress	15.13	Min. Principal Stress	-16.8

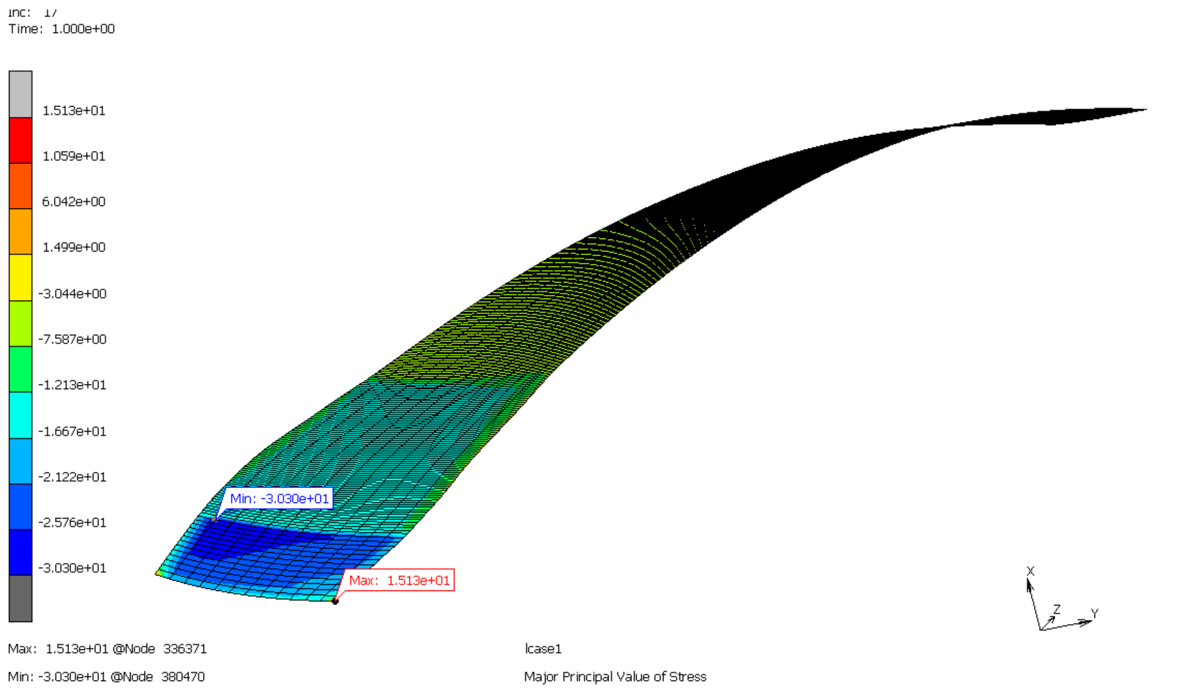

Figure 18. Minimum and maximum principal stresses - VCCT (non-Glue Breaking)

In the analyses performed on the RUZGEM 5-meter wind turbine blade, no difference was observed between VCCT and CZM. From this analysis, we understood no crack formation in VCCT. Although there was failure in this area, it was observed that there was no structural destruction. When the interface properties were entered into adhesive contact in the cohesive region with Glue Breaking, the stress values obtained more accurate results than the reference values.

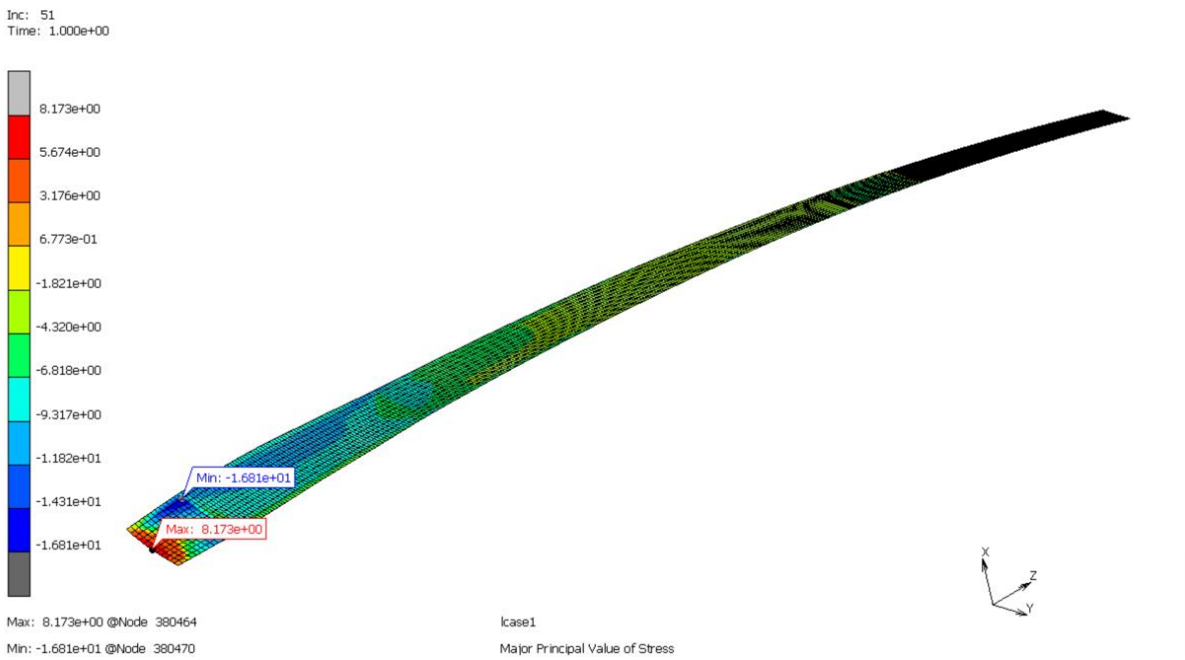

Figure 19. Minimum and maximum principal stresses - VCCT (with Glue Breaking)

3.4. Role of Compression and Principal Stress on DTU 10 MW Wind Turbine Blade

Spar cap failure may result from out-of-plane deformation caused by wind loads. This failure can manifest as transverse tensile failure in unidirectional layers closest to the neutral axis or as interlayer shear failure between layers. The typical blade arrangement, with fibers primarily aligned in the longitudinal direction, renders the spar cap relatively flexible in the lateral direction, thereby increasing the risk of transverse stress failure. Furthermore, manufacturing defects within the laminate further reduce its fatigue and ultimate strength. The +y axis is critical for this region. σ22, which is significantly high at the boundary of the delamination zone, plays a crucial role in buckling failure (Figures 20, Figure 21).

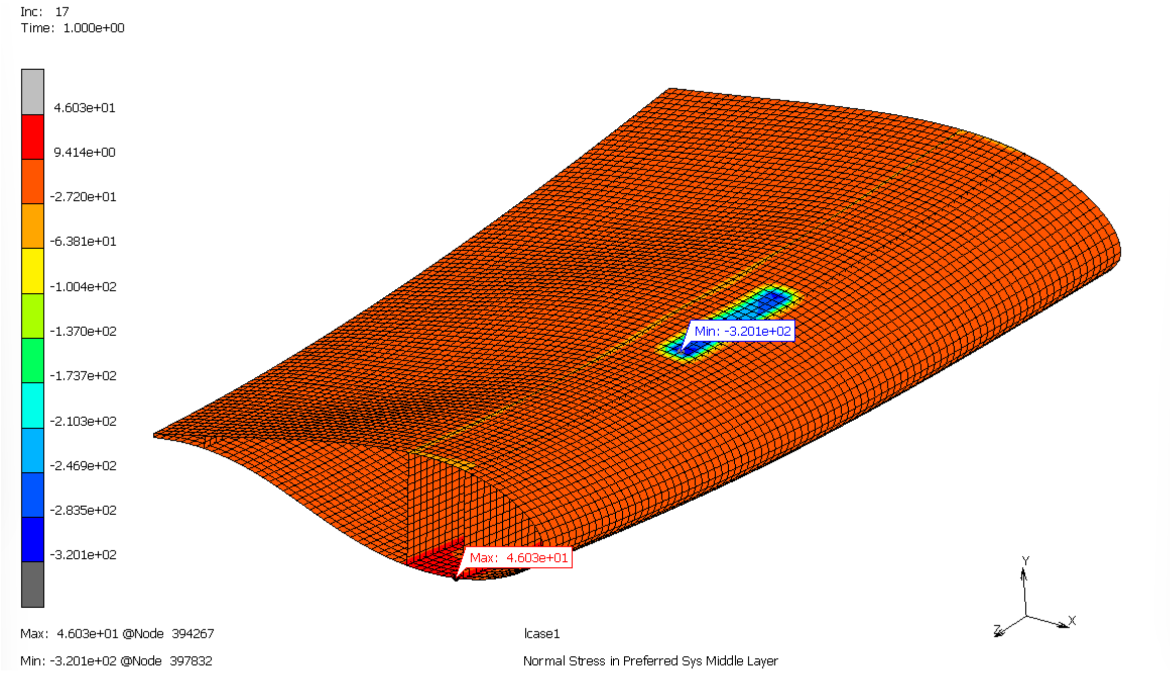

Figure 20. Normal stress in the critical region

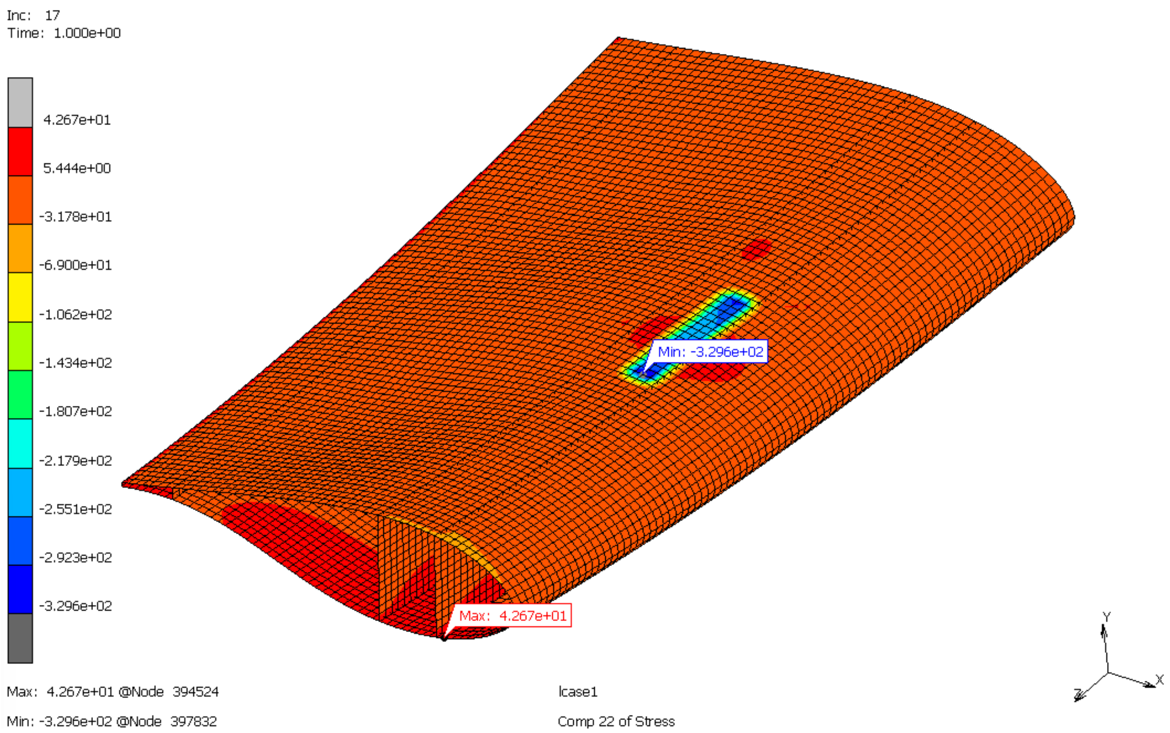

Figure 21. σ22 values in the critical region

In the context of the influence of principal stresses on blade failure, it is observed that tensile stresses predominantly affect the low-pressure surface (suction shell) of the blades, except in a specific area. This area corresponds to the blade root projection on the blade's pressure side, intersecting with the spar cap and extending to the suction side. In this specific green-colored region, compressive stresses are more prominent. Multiple factors contribute to the prevalence of compressive stresses in this area. Local buckling-induced delamination occurs in the spar cap's middle section, where the blade root compressive stresses are most pronounced (Figure 22, Figure 23).

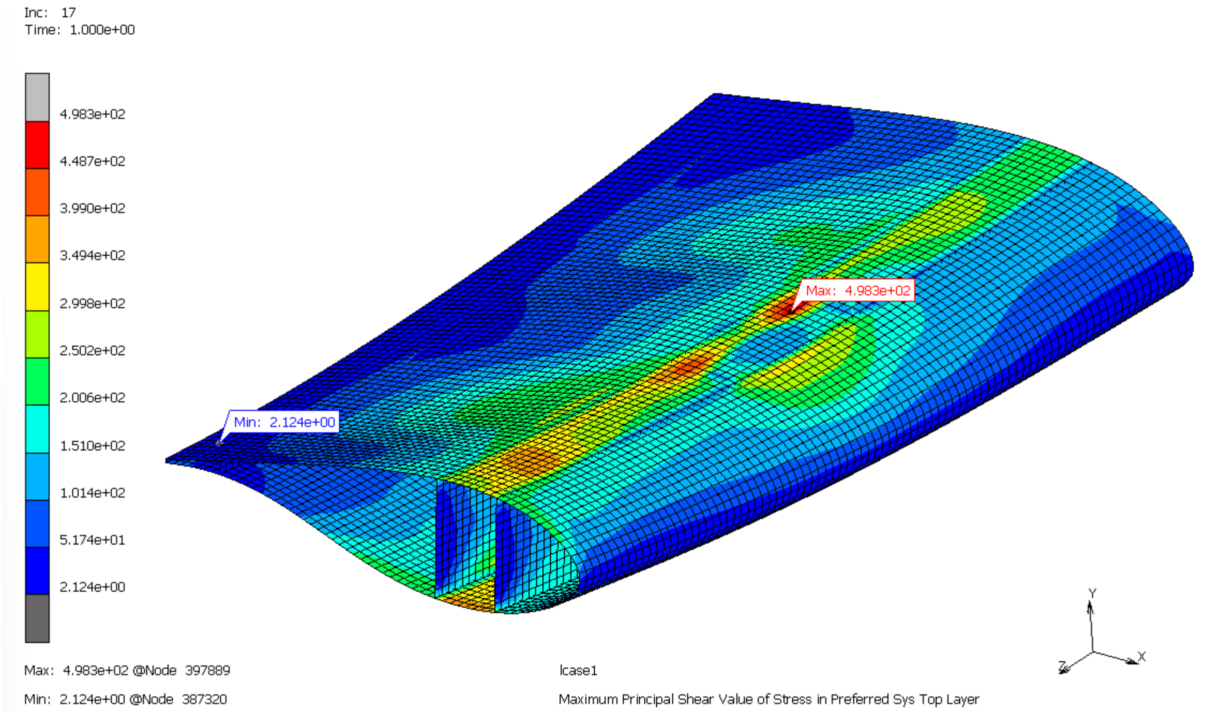

Figure 22. Maximum principal shear stresses in the critical region

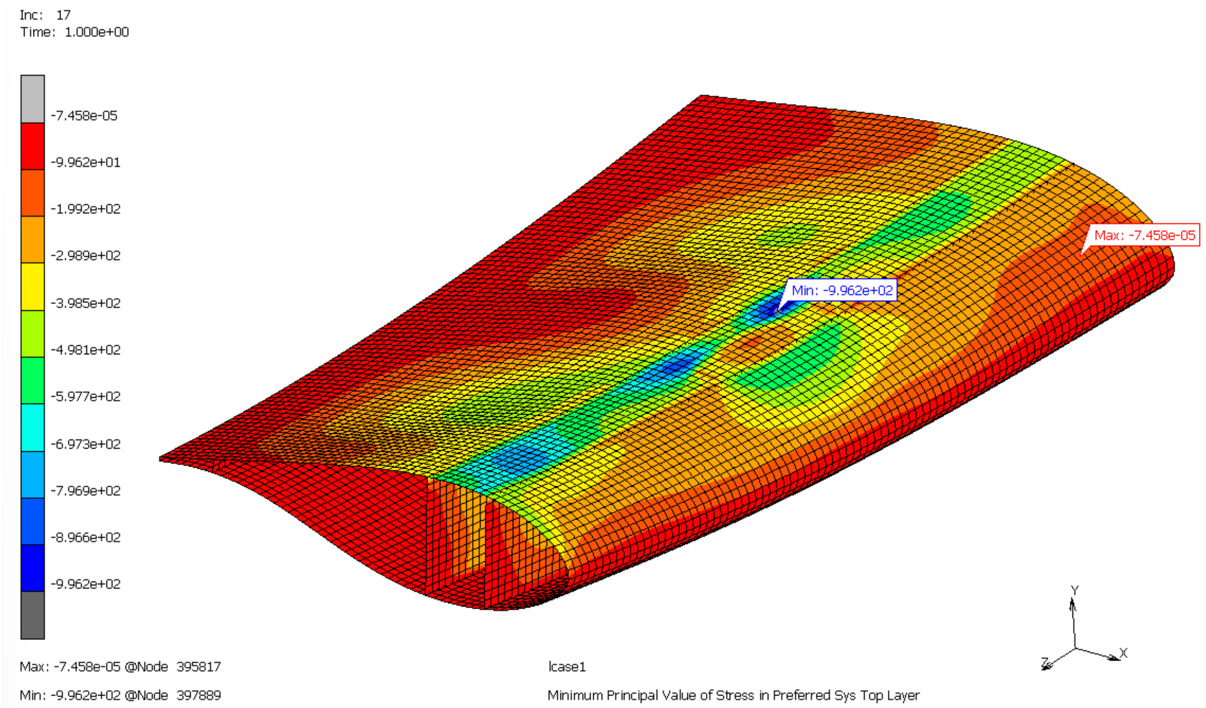

Figure 23. Minimum principal stresses in the critical region

This delamination further intensifies the stresses, subjecting the fibers to compression in two directions, potentially exceeding their tensile strength and leading to crack formation. The σ11 value, exceptionally high at the delamination boundary, significantly influences buckling fracture. The σ11 value surpasses the σ22 and σ33 values at the delimiting boundary of the material in shell models, experiencing elevated stress in the direction 1 (Figure 24).

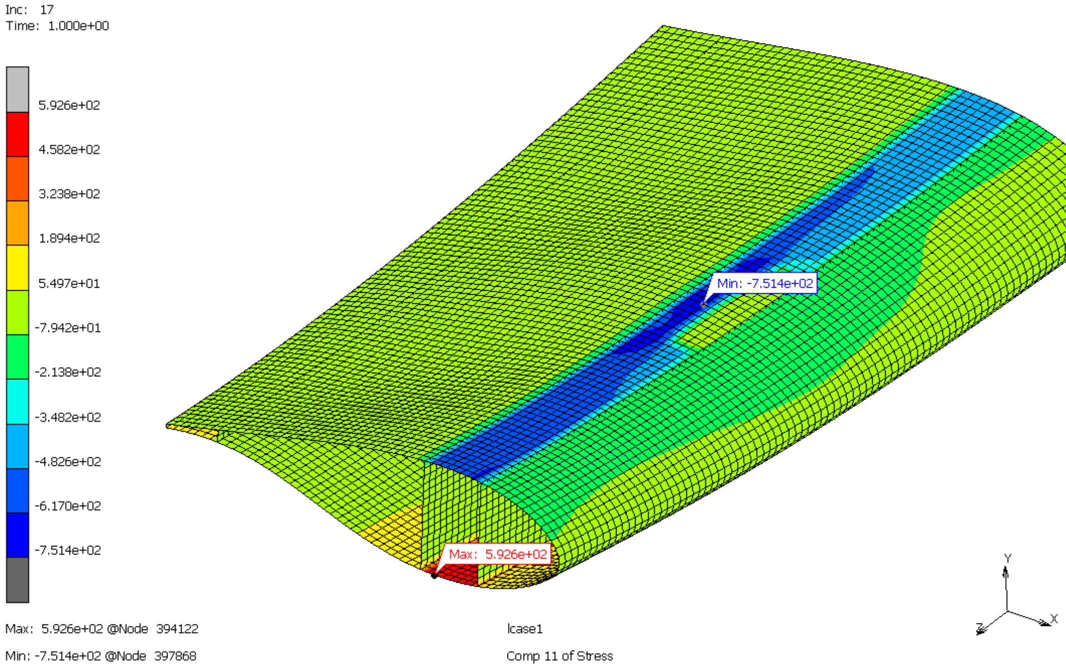

Figure 24. Effect of σ11, which has a high value at the delamination boundary on local buckling

In the central region of the delamination, the magnitudes of σ11 and σ22 surpass those of σ33, indicating that the material is subjected to more significant tensile stress along direction 1 and compressive stress along direction 2. The σ33 stress is oriented perpendicular to the fiber direction, and the layer surface exhibits a lower value (Figure 25)

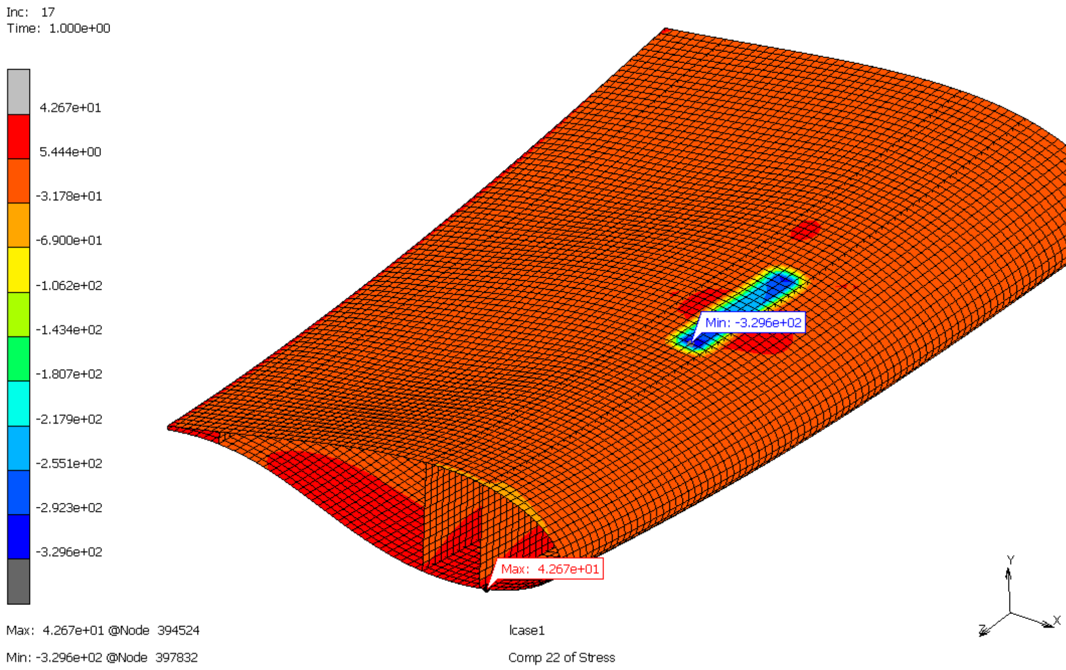

Figure 25. Compression and stress concentration along 2 directions of the fiber in the middle region of local buckling-induced delamination

The stress concentration at σ22 poses a potential risk for failure in the adhesive element. If the stress in σ22 surpasses the strength of the cohesion element, the cohesion element will fail, separating the connected parts. Here are several methods to mitigate stress concentration in σ22:

- Increase the thickness of the adhesive bonding
- Use a more resilient adhesive material
- Modify the adhesive bonding geometry to reduce stress concentration
- Add a fillet or chamfer to the edge of the adhesive joint to minimize stress concentration

3.5. Role of Total Strain Energy Density on DTU 10 MW Wind Turbine Blade

The node with the highest total strain energy density in the DTU 10MW wind turbine blade is identified as the crack initiation point, and crack formation is observed at this location (Figure 26).

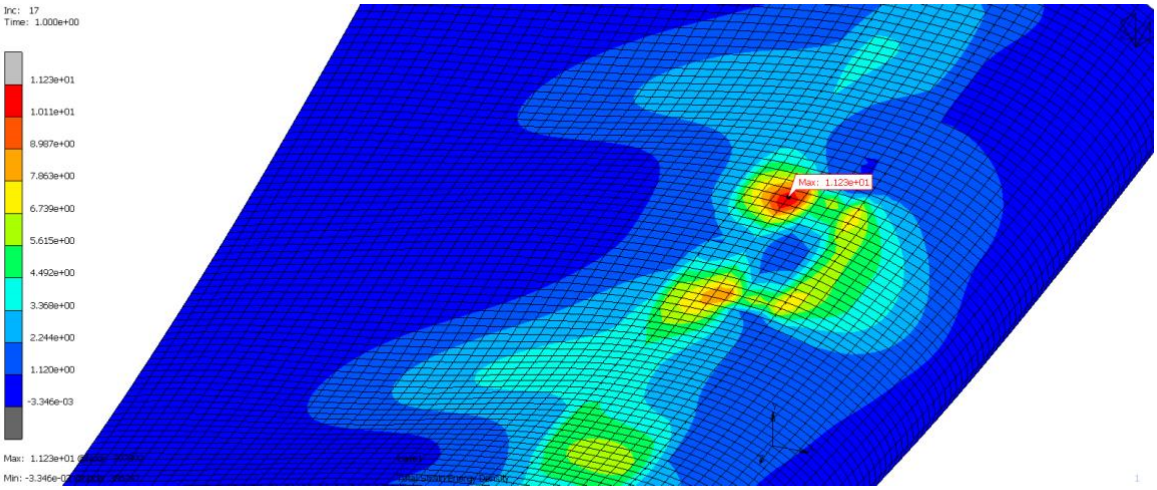

Figure 26. The node where the total strain energy density is maximum

The process of material failure involves crack initiation, growth, and coalescence, with stress concentrations occurring at the crack tip (Figure 27). The equivalent of von Mises stress at a crack is used to assess the impact of the crack on the material's durability. Fracture of the material may occur when the equivalent von Mises stress at the crack edges reaches a critical level. Once this critical value is reached, the crack significantly compromises the material's durability and poses a severe safety hazard.

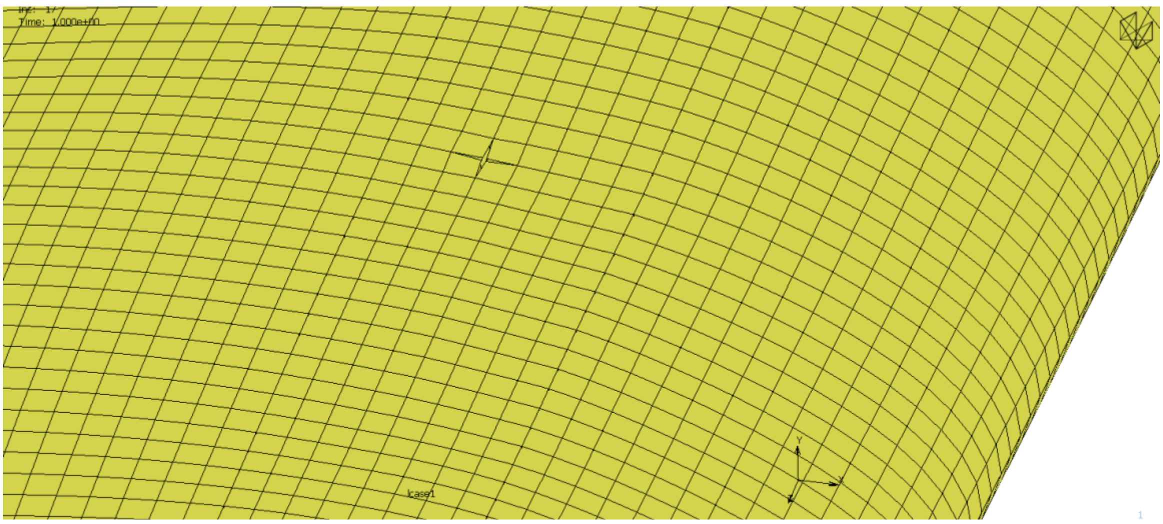

Figure 27. Crack formation at the selected node

The crack is located in the central part of the spar cap. The length and shape of the crack are crucial in determining the equivalent von Mises stress. A longer, sharper crack produces more concentrated stress at the edges, leading to a higher equivalent von Mises stress. Additionally, the stress at the crack edges diminishes significantly with distance from the crack, indicating that stress is concentrated at the edges but becomes more uniformly distributed further away from the edges (Figure 28).

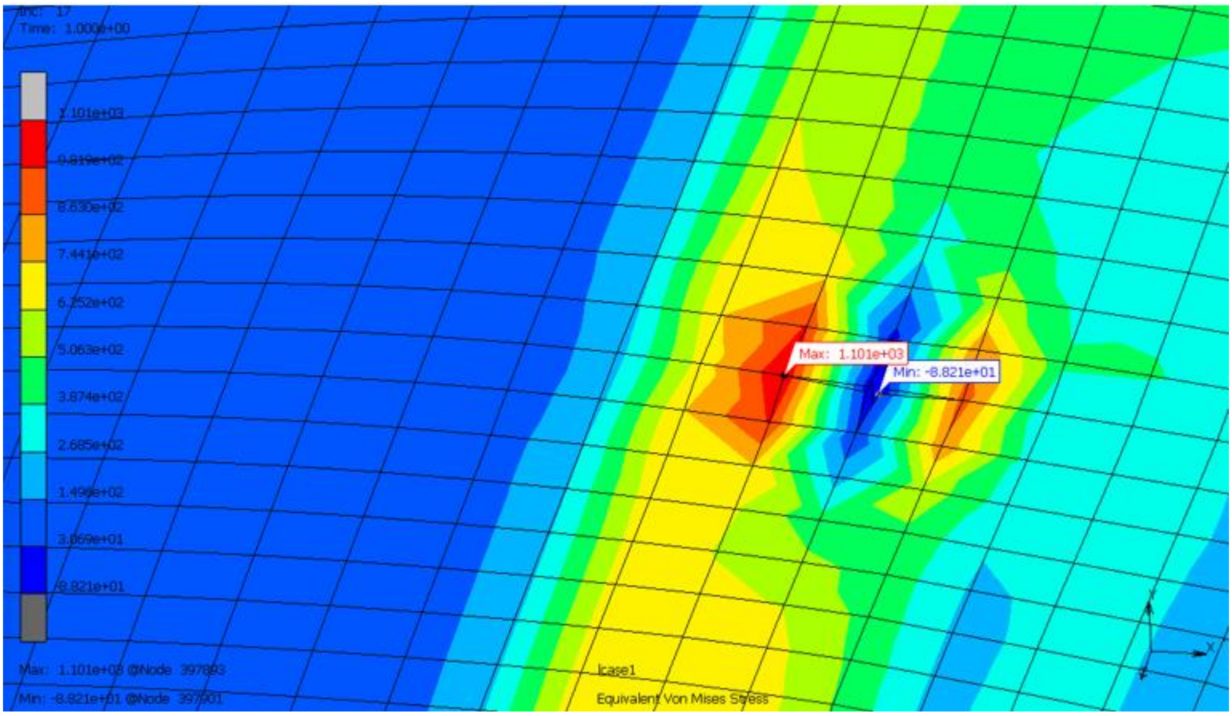

Figure 28. Equivalent von Misses stress in the crack

4. Conclusions

In this study, advanced methods from FEM simulation programs are applied within a specific scope to revisit and provide new insights into the study of Batmaz et al. (2021) and Haselbach (2015), which have made significant contributions to the literature. Extensive research has shown that turbine blades often experience failure, resulting in a significant loss of load-carrying capacity, especially when bending in the flapwise direction. The primary failure occurs in the transition zone near the root and is characterized by various failure modes caused by both in-plane and through-thickness stresses. A comprehensive analysis of the intricate failure features in the transition zone was conducted using finite element simulation with a global-local modeling approach. It was discovered that these failure features accumulate over the blade's loading history. Commonly observed failure modes included delamination of the spar cap on the suction side, separation of the sandwich surface-core bond, laminate fracture, and spar web rupture. Among these, spar cap delamination and spar web failure were identified as the primary causes of blade failure.

Wind-induced pressure generates material stresses σ11 and σ22, which are the main contributors to the buckling of spar caps. Comparing these two stresses, it is evident that σ11, with its high value at the delamination limit, is the primary cause of failure. Laminates with delamination defects exhibit local buckling and a combination of local and global buckling under heavy load. Local buckling in the delamination region, influenced by σ11, subjects the fibers in the central area of the delamination to pressure along two directions, resulting in stress concentration. Consequently, stress concentration occurs at the delamination boundary, dependent on σ11, in the direction in which the laminate bends. The adhesive bonding region, being less stiff than the surrounding material, experiences stress concentration at its edge due to the difference in stiffness. Stress concentration at σ22 represents a potential failure zone for the adhesive element. If the stress at σ22 exceeds the strength of the cohesion element, the cohesion element will rupture, separating the connected parts. In this study, the following results were observed:

1. σ11 leads to buckling, particularly in defective laminates. Increasing compressive strength along the fiber slows down buckling-induced failure in laminates.
2. There is stress concentration in the middle of the delamination area due to σ11 and σ22 along the direction.
3. σ33 has minimal impact on the buckling failure of the structure.
4. Glue Breaking continues as a Touch contact when the adhesive contact effect is removed. Incorporating this feature obtained more accurate results.
5. Total strain energy density indicates how much energy the material consumes during plastic deformation. The fact that the von Mises stress maximum is slightly further away from the total strain energy density maximum may indicate that the material is softer and more ductile at the other end of the region. In this case, even though the material in the area has high von Mises stress, the total strain energy density will be low. As a result, the difference in the regions where von Mises stress and total strain energy density are concentrated may result from the difference in the material properties of the area, the applied load, or the form factor.
6. Crack formation is anticipated to occur predominantly in the region where the overall strain energy density is concentrated. Additionally, observations indicated the disappearance of the contact condition in both the area where adhesive separation was anticipated and the portion where laminate breakage was expected.
7. No visible cracks were detected, likely due to compressive forces. Tensile stresses typically lead to crack formation, whereas compressive stresses tend to prevent cracks from widening. The drop in ply along the material layout, attributed to the addition of the spar in this area, is the primary factor contributing to the separation failure observed here. Furthermore, it should be noted that delamination does not necessarily equate to "fracture." Instead, it is just one of the potential factors that can contribute to structural failure.

The rapid advancement of FEM programs clearly indicates that future studies building on this study will be highly beneficial for gaining a deeper understanding of failure mechanisms. Future studies could include the following: creating 3D models to analyze delamination more comprehensively or dividing the examined blade structure into sub-models for more specific analyses using newly developed FEM tools such as shell-to-shell, shell-to-solid, and solid-to-solid connection tools.

Author Statement

The authors confirm equal contribution to the paper.

Conflict of Interest

The authors declare no conflict of interest.

References

Bak, C., Zahle, F., Bitsche, R., Kim, T., Yde, A., Henriksen, L. C., Hansen, M. H., Blasques, J. P. A. A., Gaunaa, M., & Natarajan, A. (2013). The DTU 10-MW Reference Wind Turbine. *In Danish Wind Power Research 2013* - Trinity, Fredericia, Denmark.

Batmaz, O. A., Muyan, C., & Çöker, D. (2019). Rüzgar Türbin Kanatlarında Yapıştırıcı Ayrılma Hasarının Kanat Yapısal Bütünlüğüne Etkisi. In 6. İzmir Rüzgâr Sempozyumu, 23-24 Eylül, 2021.

Branner, K., & Berring, P. (2011). Compressive Strength of Thick Composite Panels. *In Risø National International Symposium on Material Science*.

Castro, O., & Branner, K. (2021). Effect Of Tunneling Cracks on Structural Property Degradation of Wind Turbine Blades.

Chen, X., Qi, Z., Yang, K., Zhao, X., & Xu, J. (2015). Numerical Analysis and Experimental Investigation of Wind Turbine Blades with Innovative Features: Structural Response and Characteristics. *Science China Technological Sciences*.

Chen, X., Zhao, W., Zhao, X. L., & Xu, J. Z. (2014). Failure Test and Finite Element Simulation of a Large Wind Turbine Composite Blade Under Static Loading. *Energies*.

Haselbach, P. U. (2015). The Ultimate Strength of Wind Turbine Blades Under Multiaxial Loading. *Technical University of Denmark*.

Haselbach, P. U., & Branner, K. (2016). Initiation of Trailing Edge Failure in Full-Scale Wind Turbine Blade Test. *Engineering Fracture Mechanics*.

Mankins, J. C. (2023). Technology Readiness Levels. In Marc, MSC. User's Guide, Volume A: *Theory and User Information* (MSC Software Corporation).

Muyan, C., & Çöker, D. (2020). Strength Analysis of a 5-M Composite Wind Turbine Blade Under Static and Fatigue Loading Conditions. *In IOP Conference Series: Materials Science and Engineering.*

Overgaard, L. C. T., & Lund, E. (2010). Structural Collapse of a Wind Turbine Blade. Part A: Static Test and Equivalent Single Layered Models. *Composites Part A*, 41.

Yang, J., Peng, C., Xiao, J., Zeng, J., Xing, S., Jin, J., & Deng, H. (2012). Structural Investigation of Composite Wind Turbine Blade Considering Structural Collapse in Full-Scale Static Tests.